



How does fusion hindrance show up in medium-light systems? The case of $^{48}\text{Ca} + ^{48}\text{Ca}$

A.M. Stefanini^{a,*}, G. Montagnoli^b, R. Silvestri^a, L. Corradi^a, S. Courtin^c, E. Fioretto^a, B. Guiot^a, F. Haas^c, D. Lehbertz^c, P. Mason^b, F. Scarlassara^b, S. Szilner^d

^a INFN, Laboratori Nazionali di Legnaro, I-35020 Legnaro (Padova), Italy

^b Dipartimento di Fisica, Università di Padova, and INFN, Sezione di Padova, I-35131 Padova, Italy

^c IPHC, CNRS-IN2P3, Université de Strasbourg, F-67037 Strasbourg Cedex 2, France

^d Ruđer Bošković Institute, HR-10002 Zagreb, Croatia

ARTICLE INFO

Article history:

Received 9 May 2009

Received in revised form 24 June 2009

Accepted 10 July 2009

Available online 17 July 2009

Editor: V. Metag

PACS:

25.70.Jj

24.10.Eq

Keywords:

Heavy-ion fusion

Sub-barrier cross sections

Coupled-channels model

ABSTRACT

The fusion excitation function of $^{48}\text{Ca} + ^{48}\text{Ca}$ has been measured above and well below the Coulomb barrier, thereby largely extending the energy range of a previous experiment down to very low cross sections. This system has a negative Q -value for compound nucleus formation. The fusion cross section decreases steadily below the barrier with no conspicuous change of slope below $\simeq 300 \mu\text{b}$. Coupled-channels calculations using a Woods–Saxon potential indicate that a large diffuseness parameter is needed to reproduce the sub-barrier cross sections. A close analogy with the case of $^{36}\text{S} + ^{48}\text{Ca}$, with $Q > 0$, is pointed out. The sign of the Q -value does not influence fusion cross sections down to the 300–600 nb level.

© 2009 Elsevier B.V. All rights reserved.

1. Introduction

The behavior of heavy-ion fusion excitation functions at energies near and well below the Coulomb barrier, continues to be a matter of wide experimental and theoretical interest. Several years ago, limitations to fusion for heavy systems were found, in extensive research performed mainly at GSI aiming to explore the possibility of producing superheavy elements (see e.g. the reviews of Refs. [1,2]). In particular, measurements for some systems like $\text{Zr} + \text{Zr}$ [3] revealed that the excitation function below the barrier drops very rapidly, with a logarithmic slope much larger than predicted by tunnelling calculations using conventional ion–ion potentials.

More recently, it has been observed also for several medium-heavy systems [4,5] that when decreasing the energy below the lower threshold of the distribution of fusion barriers [6], produced by channel couplings, the logarithmic slope of the excitation function $L(E)$ does not saturate, rather it keeps increasing. One finds

that the measured cross sections fall well below the predictions of standard coupled-channels (CC) calculations using a nuclear interaction with a Woods–Saxon shape. In all of these systems, when decreasing the energy, $L(E)$ reaches and undoubtedly crosses the value $L_{\text{CS}}(E)$ expected for a constant astrophysical S -factor [7,8] which, as a result, develops a maximum at the crossing energy E_s . In these experiments, this crossing was taken as a phenomenological signal for fusion “hindrance”, where E_s conventionally marked its threshold.

In the case of $^{16}\text{O} + ^{208}\text{Pb}$ [9] the low-energy slope is very steep but almost saturates at $\simeq L_{\text{CS}}(E)$. It was argued that the coherent coupled-channels model is inadequate, and that a gradual onset of decoherence takes place with increasing overlap of the two nuclei. Though the model based on the incompressibility of nuclear matter when the density overlap is large [10,11], has been very successful for several systems, we are still far, generally speaking, from a complete understanding of fusion cross sections at far sub-barrier energies. Fusion “hindrance” shows many facets, reflecting different physical situations.

In the light systems of astrophysical interest (e.g. $^{12}\text{C}, ^{16}\text{O} + ^{16}\text{O}$, see [12]), $L(E)$ tends to become parallel to $L_{\text{CS}}(E)$ and, as a consequence, a conclusion on the presence of hindrance in these

* Corresponding author.

E-mail address: alberto.stefanini@lnl.infn.it (A.M. Stefanini).

cases is less unambiguous, but would be very important [13] from the point of view of nucleosynthesis rates during the oxygen and carbon burning stages in stars (see [14,15] and references therein).

Medium-light systems are a bridge between the light and the heavy ones, and can provide us with interesting information on hindrance. A first issue raised has been the possible role of Q -value for compound nucleus (CN) formation in the low-energy region of the excitation function. It is straightforward to show [5] that with $Q > 0$ a crossing between $L(E)$ and $L_{CS}(E)$ is not algebraically necessary, that is, the S -factor may not show any maximum at whichever energy. Now, the Q -value is always positive in light systems and negative in medium-heavy and heavy ones. Two recent experiments were performed for medium-light systems with $Q > 0$ with the aim of revealing their low-energy behavior. For the first case $^{28}\text{Si} + ^{30}\text{Si}$ [16] ($Q = +14.3$ MeV), the excitation function could be measured only down to $\simeq 40$ μb , and a clear-cut conclusion on the existence of a maximum of S is difficult. The system $^{36}\text{S} + ^{48}\text{Ca}$ ($Q = +7.6$ MeV) was the object of the second study [17]. Down to $\sigma_{\text{fus}} \simeq 600$ nb, a steady decrease of the fusion cross sections was observed for this system with no pronounced change of slope below the barrier. The logarithmic derivative saturates and does not reach $L_{CS}(E)$. Nevertheless, CC calculations using a Woods–Saxon potential can only reproduce the data with a large diffuseness parameter $a = 0.95$ fm.

The case of $^{48}\text{Ca} + ^{48}\text{Ca}$ is a very interesting nearby case with negative Q -value ($Q = -2.99$ MeV). As shown in Ref. [17] (Fig. 5 of that paper), the available data for this system [18] show that the slope of its excitation function is very similar to the case of $^{36}\text{S} + ^{48}\text{Ca}$, down to the lowest measured energy for $^{48}\text{Ca} + ^{48}\text{Ca}$ (where $\sigma = 150$ μb). This energy, however, is too high to allow any reasonable extrapolation into the interesting region at still lower energies. Therefore we found very attractive to extend the measurement of fusion cross sections in $^{48}\text{Ca} + ^{48}\text{Ca}$, so to test whether the sign of the Q -value has a role or not in a wider energy region. Extending the measurements for $^{48}\text{Ca} + ^{48}\text{Ca}$ is also interesting in itself for the dynamics of near-barrier fusion, where nuclear structure (we have two very stiff and neutron-rich magic nuclei) is expected to determine fusion cross sections and to characterize the barrier distribution.

This Letter is dedicated to the results of this experiment. Several high-energy points (above the barrier) have been also re-measured, in the range where the previous data show some oscillations, and a particular experimental care has been devoted to the absolute cross section scale. The re-measured cross sections above the barrier are in good agreement with the systematics of Ref. [19].

The experimental set-up and procedures are discussed in Section 2, and are followed by a presentation of the new data and in particular of the low-energy trend of the excitation function. Then the results of coupled-channels calculations are reported (Section 3), and a comparison is done with the aforementioned case $^{36}\text{S} + ^{48}\text{Ca}$ in Section 4. Section 5 summarizes the main results of the present work.

2. Experiment and results

The present measurements have been performed at the Laboratori Nazionali di Legnaro of INFN using the same set-up and procedures as for the previous ones [17] on $^{36}\text{S} + ^{48}\text{Ca}$. Here a short account of experimental conditions is given, and we refer to that recent paper for further details and examples of experimental results. A metallic calcium sample, enriched to $\simeq 65\%$ in mass 48, was sprayed with ammonia and the resulting CaH^- ions were injected into the XTU Tandem. The accelerated ^{48}Ca beams, in the

energy range 93–122 MeV with intensities 5–10 pA, were focused onto $^{48}\text{CaF}_2$ targets 50 $\mu\text{g}/\text{cm}^2$ thick (evaporated on carbon backings 10 $\mu\text{g}/\text{cm}^2$ thick). The beam purity, besides the strict selection achieved by the combined accelerating voltage and the 90° high-energy deflection magnet, is determined *a priori* by the 1/200 mass resolution of the 90° injecting magnet out of the ion source. This excludes the contamination of lighter calcium isotopes in the injected beam. In any case, the magnet field was scanned (as usually done) up and down before the experiment, so to clearly recognize the mass spectrum of calcium isotopes, and set up for ^{48}Ca . The only other stable nuclide with $A = 48$ is ^{48}Ti , with a higher Z .

Four silicon detectors monitored the beam by measuring its elastic scattering from the target. They were placed above and below, and to the left and right of the beam at the same scattering angle $\theta_{\text{lab}} = 16^\circ$. The beam energy losses in the targets were taken into account, as well as the calcium isotopic enrichment (91.8% in mass 48), with a predominant 7.7% impurity of ^{40}Ca (see Ref. [17]). In the laboratory system, the barrier for $^{48}\text{Ca} + ^{40}\text{Ca}$ is $\simeq 13$ MeV higher than for $^{48}\text{Ca} + ^{48}\text{Ca}$. The impurity of ^{46}Ca (nearest to ^{48}Ca) is $< 0.01\%$ with a barrier difference of $\simeq 3$ MeV. All this produces only negligible corrections even for the lowest energies where the experimental errors are rather large. Concerning possible target contaminations with $Z < 20$, the only non-negligible component is a < 1000 ppm silicon impurity which, however, would produce evaporation residues (ER) much lighter than ^{48}Ca , easily separated out by means of the combined energy-time of flight measurement (see below).

The recoiling ER were spatially separated from the transmitted beam and beam-like particles at 0° and at small angles by an electrostatic deflector [20]. The beam ions were stopped at the exit of the deflector, while ER were detected by means of an energy time-of-flight telescope composed of two micro-channel plate detectors followed by a 600 mm² silicon surface-barrier detector [17], covering a geometrical solid angle $\simeq 82$ μsr . The ER yields were normalized to the average Mott scattering cross section into the four monitor detectors. Fusion-fission is negligible for the present system, so that total fusion cross sections were derived from the normalized 0° ER yields, from the ER angular distributions measured in the previous experiment [18], and from the transmission of the electrostatic deflector $T = 0.75 \pm 0.03$, derived from systematic measurements performed for systems with nearby masses and mass asymmetries [17,20–22]. The absolute cross section scale is estimated to be accurate within $\pm 7\%$. Indeed, special care has been taken to check the whole set-up, and to measure the solid angle of all detectors by placing an α -source at the target position.

The high-energy part of the fusion excitation function measured in this work and its comparison with the results of Ref. [18], are shown in Fig. 1 (upper panel) in a linear scale. The present fusion cross sections are much smaller than the previous ones in the region $\sigma \simeq 50$ –250 mb. A good overall agreement can be found if the older data are scaled down by 20%, as plotted in the figure. The oscillations reported in Ref. [18] are not observed in the present data, where the high-energy cross sections show a quite smooth behavior vs. energy (see also the bottom panel of Fig. 1).

We point out that the present data at energies above the barrier are in much better agreement with the systematics of Newton et al. [19]. Merging the two data sets allows to extract an updated representation of fusion barrier distribution, from the second energy derivative of $E\sigma$ [6], using the three-point difference [23] formula with an energy step of 1.6 MeV. The very rigid structure of the two nuclei produces a single peak at $\simeq 51$ MeV [24], as reported in Fig. 2 (top panel).

Additionally, it is useful to examine of the trend of the logarithmic slope of the excitation function, plotted in the bottom panel of Fig. 2. The experimental slope increases around and below the bar-

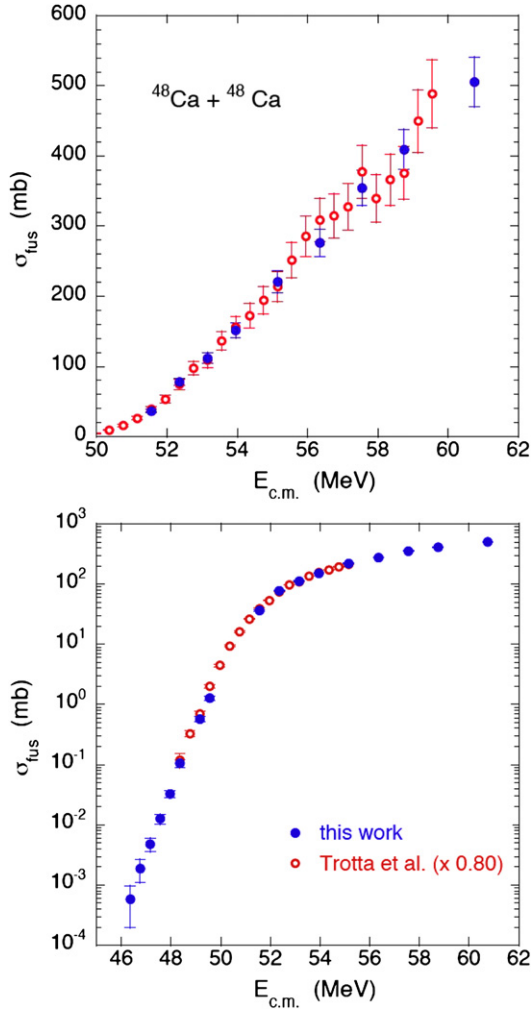


Fig. 1. (Color online.) Fusion excitation function of $^{48}\text{Ca} + ^{48}\text{Ca}$, as measured in the present work and as reported by Trotta et al. [18]. Total errors (statistical plus systematic ones, see text) are plotted in the top panel. Only statistical uncertainties are reported in the bottom panel. Here the previous data are shown only up to 55 MeV, for the sake of clarity.

rier but a saturation shows up below $\simeq 48.5$ MeV. The slope does not reach L_{CS} and tends to become parallel to it with decreasing energy, in a close analogy with the case of $^{36}\text{S} + ^{48}\text{Ca}$ [17]. Consequently, the S -factor does not show any maximum in the measured energy range for both systems.

3. Coupled-channels calculations

The excitation function of $^{48}\text{Ca} + ^{48}\text{Ca}$ has been compared with the results of coupled-channels (CC) calculations performed with the CCFULL code [25] using the Woods–Saxon parametrization of the nuclear potential, and modified for symmetric systems [26]. The low-lying 2^+ and 3^- vibrational states of ^{48}Ca were included in the calculations, as well as their mutual excitations. ^{48}Ca is very stiff, with the 2^+ (3^-) state at 3.832 (4.507) MeV and deformation parameter $\beta = 0.11$ (0.23) [27].

We stress that it is not our aim to attain the best fit of the data, rather we like to give indications for future theoretical work. We show the results obtained with two different bare potentials. The first one is essentially the Akyüz–Winther (AW) potential [28] (giving good results in the analysis of the previous data [18]). The geometry is the same one with $r_0 = 1.18$ fm and $a = 0.66$ fm. Only the well depth has been slightly re-adjusted, so to give a barrier

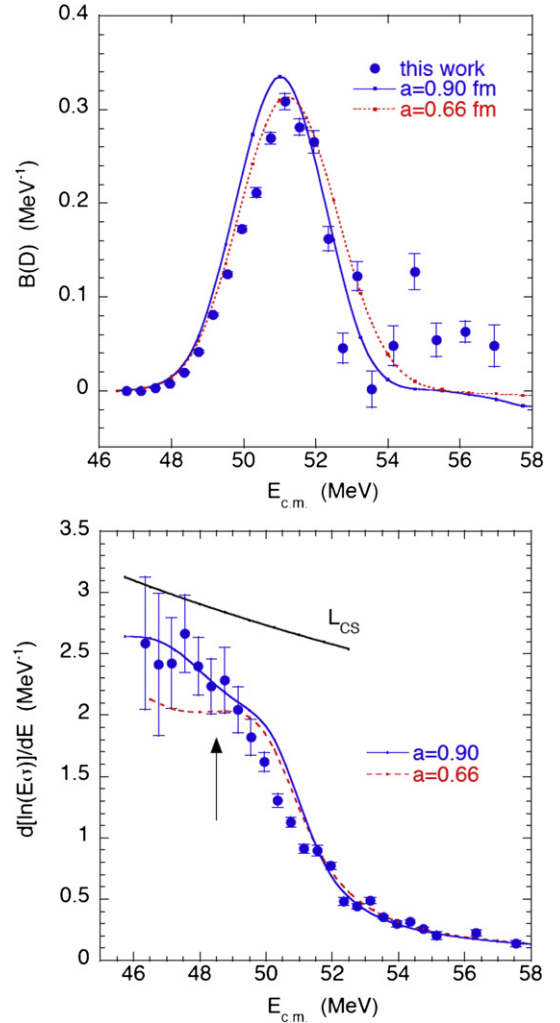


Fig. 2. (Color online.) (top) The fusion barrier distribution of $^{48}\text{Ca} + ^{48}\text{Ca}$ as extracted from the data, together with the results of CC calculations; (bottom) logarithmic derivative of $E\sigma$ with respect to the energy. The experimental points are the incremental ratios for successive pairs of measured points, with purely statistical uncertainties. The arrow marks the lowest energy measured previously [18]. This shows the importance of the additional points measured in this work, for the determination of the low-energy trend of the excitation function.

height $V_b = 52.2$ MeV, that is, 0.6 MeV higher than the AW value. This takes care of the fact that the previous cross sections have been scaled down by the factor 0.80, as discussed above.

The second potential has a much larger diffuseness parameter $a = 0.90$ fm and r_0 has been reduced to 1.05 fm, so to give approximately the same barrier V_b with a well depth $V_0 = 84.9$ MeV. The total ion–ion potential (nuclear plus Coulomb) is shallower than the first one, nevertheless its internal pocket (for $l = 0$) is $\simeq 38$ MeV deeper than the lowest measured energy. The large diffuseness of this potential makes it similar to the one used for $^{36}\text{S} + ^{48}\text{Ca}$ [17], that allowed to reproduce those data both above and below the barrier.

No imaginary component of the potential is included in this version of CCFULL. Both real potentials, described here above, produce a barrier distribution quite similar to the experimental one, when couplings are included. This is shown in Fig. 2 (top). The excitation function of $^{48}\text{Ca} + ^{48}\text{Ca}$, as resulting from the combination of the previous and present data sets, is compared with calculations in Fig. 3. In the top panel the cross sections are plotted in a linear scale that shows better the trends above the barrier. The two

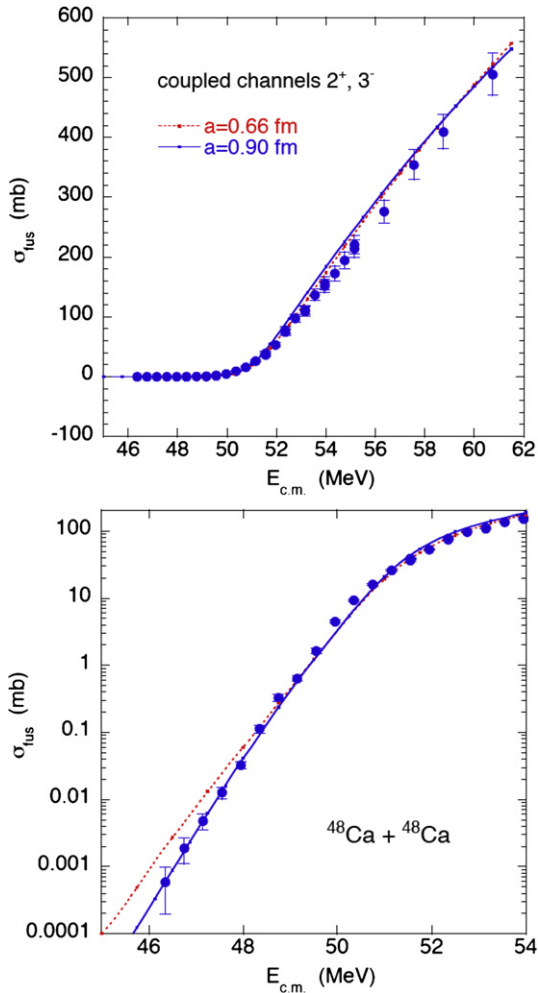


Fig. 3. (Color online.) (top) Fusion excitation function of $^{48}\text{Ca} + ^{48}\text{Ca}$. The cross section scale is linear, and the errors are total uncertainties. (bottom) The same data in a logarithmic scale; only statistical uncertainties are reported here.

CC calculations give very similar results in this energy range. Both of them overestimate the data slightly, but well within the experimental errors. The situation is changed below the barrier (see bottom panel), where it is clear that the “AW-like” potential gives a wrong slope (too flat), while the calculation with $a = 0.90$ fm fits the data much better. It is worth noting that the present low-energy points (the five lowest points) are essential for a clear-cut discrimination between the two calculations.

Analogous conclusions may be drawn by considering the logarithmic slopes of the excitation function, plotted in Fig. 2 vs. energy (bottom panel). There, the slope expected for a constant S-factor L_{CS} is also reported for reference. The calculation with $a = 0.90$ fm gives a good fit of the low-energy slope, whereas the slope calculated with $a = 0.66$ fm is well below the data, although the errors are rather large for the relevant points.

4. Comparison with $^{36}\text{S} + ^{48}\text{Ca}$

It is interesting to compare the behavior of $^{48}\text{Ca} + ^{48}\text{Ca}$ with the results of the recent measurements for $^{36}\text{S} + ^{48}\text{Ca}$ [17]. The two excitation functions are reported in Fig. 4 (top panel). The energy scale is relative to the barrier height, taken as the value given by the bare potential with large diffuseness used in this work ($V_b = 51.9$ MeV) and in Ref. [17] for $^{36}\text{S} + ^{48}\text{Ca}$ ($V_b = 43.3$ MeV). The ordinate is not corrected for the small difference in barrier

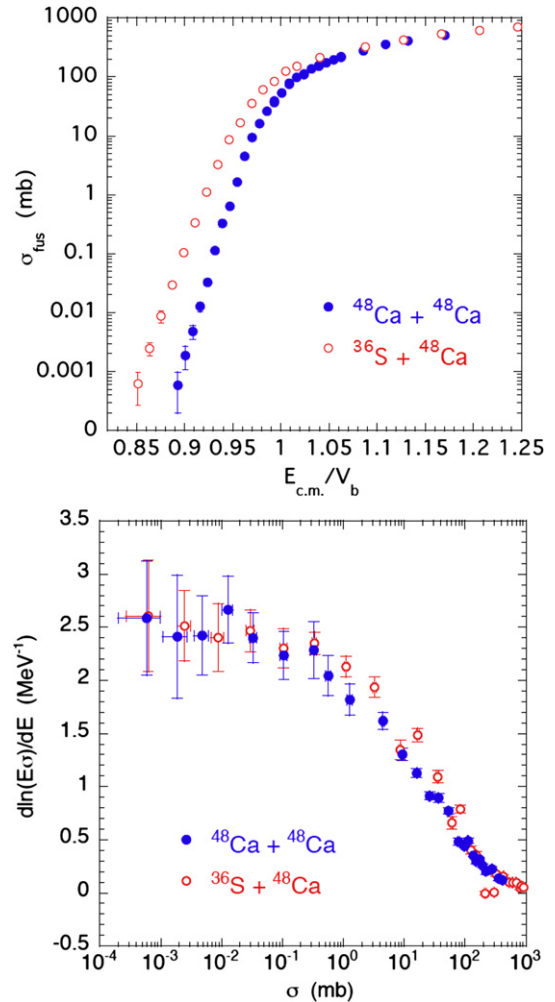


Fig. 4. (Color online.) (top) Fusion excitation functions of $^{36}\text{S} + ^{48}\text{Ca}$ and of $^{48}\text{Ca} + ^{48}\text{Ca}$ in a reduced energy scale. (bottom) Logarithmic derivatives of $E\sigma$ vs. fusion cross sections. This representation eliminates trivial Coulomb barrier differences.

position R_b . The two excitation functions are very similar to each other. The relative enhancement of $^{36}\text{S} + ^{48}\text{Ca}$ below the barrier is due to the stronger quadrupole and octupole vibrations in this system.

The comparison of the low-energy slopes reveals in more detail the striking similarity between the two systems. Fig. 4 (bottom) indicates that the two slopes, after a sharp increase just below the Coulomb barrier, level off and become pretty constant with decreasing cross section as a function of energy. Since the Q -value for CN formation has opposite signs in the two systems, this parallel behavior seems to invalidate the previous speculative hypothesis that the slope saturation may be due to the positive Q of $^{36}\text{S} + ^{48}\text{Ca}$, at least in the measured energy range.

However, we are left with the problem of understanding the underlying physics, since slightly heavier systems like $^{58}\text{Ni} + ^{58}\text{Ni}$ or $^{64}\text{Ni} + ^{64}\text{Ni}$ [29] do show a continuously increasing slope below the barrier. Indeed, the two cases $^{36}\text{S}, ^{48}\text{Ca} + ^{48}\text{Ca}$ appear to be more similar to the very light systems of astrophysical interest.

5. Summary and conclusions

This work has reported the results of measurements of fusion cross sections for $^{48}\text{Ca} + ^{48}\text{Ca}$, extending the available data down to $\sigma \simeq 500$ nb. Merging the present and previous data sets produces a very regular excitation function down to the lowest measured

energies. Its slope increases only slightly below $\simeq 48.5$ MeV and remains, anyway, below the L_{CS} value, so that no maximum of the S -factor vs. energy shows up. The present new data are essential for revealing this behavior. Above the barrier, standard CC calculations using a Woods–Saxon potential reproduce the data quite reasonably, when the low-lying quadrupole and octupole excitations are included. However, a large diffuseness parameter $a = 0.90$ fm has to be used in order to fit the data well below the barrier. An AW geometry of the bare potential with $a = 0.66$ fm results in underpredicting the low-energy slope very clearly for cross sections smaller than $\approx 300 \mu\text{b}$.

All of these features concerning $^{48}\text{Ca} + ^{48}\text{Ca}$ resemble very closely the behavior of $^{36}\text{S} + ^{48}\text{Ca}$ that was studied recently [17]. Since the Q -value for CN formation is negative in $^{48}\text{Ca} + ^{48}\text{Ca}$ ($Q = -3.0$ MeV) and positive in $^{36}\text{S} + ^{48}\text{Ca}$ ($Q = +7.6$ MeV) the very similar low-energy trend of fusion in these two systems cannot be ascribed to the sign of the Q -value, as conjectured earlier for $^{36}\text{S} + ^{48}\text{Ca}$.

Fusion hindrance should generally be associated to very steep slopes of the excitation function well below the Coulomb barrier, when standard CC calculations are taken as reference. In this sense, medium-light systems like $^{48}\text{Ca} + ^{48}\text{Ca}$ (and $^{36}\text{S} + ^{48}\text{Ca}$ as well) do show hindrance, even if no maximum of the S -factor appears in the measured energy range, since the logarithmic slopes saturate below the L_{CS} value. Further theoretical analyses would be strongly needed for unveiling the reason why slightly heavier systems like $^{58}\text{Ni} + ^{58}\text{Ni}$ or $^{64}\text{Ni} + ^{64}\text{Ni}$ behave differently, i.e. the slopes of the excitation functions steadily increases down to very small cross sections. Detailed nuclear structure effects should be possibly examined. The expression “fusion hindrance” covers a wide range of behaviors for different mass ranges and different nuclear structure situations.

Acknowledgements

We acknowledge the professional work of the XTU Tandem staff during the experiments, and Mr. M. Loriggiola for preparing targets of excellent quality. This work was partially supported by the European Commission within the 6th Framework Program through I3-EURONS (contract No. RII3-CT-2004-506065).

References

- [1] K.-H. Schmidt, W. Morawek, Rep. Prog. Phys. 54 (1991) 949.
- [2] W. Reisdorf, Phys. G: Nucl. Part. Phys. 20 (1994) 1297.
- [3] J.G. Keller, et al., Nucl. Phys. A 452 (1986) 173.
- [4] C.L. Jiang, et al., Phys. Rev. Lett. 89 (2002) 052701.
- [5] C.L. Jiang, et al., Phys. Rev. C 73 (2006) 014613;
C.L. Jiang, et al., in: L. Corradi, et al. (Eds.), Proc. Int. Conf. on Reaction Mechanisms and Nucl. Structure at the Coulomb Barrier, FUSION06, 19–23 March 2006, S. Servolo (Venice), AIP Conference Proceedings, vol. 853, AIP, New York, 2006, p. 63.
- [6] N. Rowley, G.R. Satchler, P.H. Stelson, Phys. Lett. B 254 (1991) 25.
- [7] C.L. Jiang, et al., Phys. Rev. C 69 (2004) 014604.
- [8] E.M. Burbidge, G.R. Burbidge, W.A. Fowler, F. Hoyle, Rev. Mod. Phys. 29 (1957) 547.
- [9] M. Dasgupta, et al., Phys. Rev. Lett. 99 (2007) 192701.
- [10] Ş. Mişicu, H. Esbensen, Phys. Rev. Lett. 96 (2006) 112701.
- [11] Ş. Mişicu, H. Esbensen, Phys. Rev. C 75 (2007) 034606.
- [12] C.L. Jiang, B.B. Back, R.V.F. Janssens, K.E. Rehm, Phys. Rev. C 75 (2007) 057604.
- [13] C.L. Jiang, in: K.E. Rehm, B.B. Back, H. Esbensen, C.J. Lister (Eds.), Proc. Int. Conf. on New Aspects of Heavy Ion Collisions Near the Coulomb Barrier, Fusion08, Chicago, Illinois, 22–26 September 2008, AIP Conference Proceedings, vol. 1098, 2009, p. 145.
- [14] C.L. Jiang, K.E. Rehm, B.B. Back, R.V.F. Janssens, Phys. Rev. C 79 (2009) 044601.
- [15] L.R. Gasques, et al., Phys. Rev. C 76 (2007) 035802.
- [16] C.L. Jiang, et al., Phys. Rev. C 78 (2008) 017601.
- [17] A.M. Stefanini, et al., Phys. Rev. C 78 (2008) 044607.
- [18] M. Trotta, et al., Phys. Rev. C 65 (2001) 011601.
- [19] J.O. Newton, et al., Phys. Rev. C 70 (2004) 024605;
J.O. Newton, et al., Phys. Lett. B 586 (2004) 219.
- [20] A.M. Stefanini, et al., Phys. Rev. Lett. 74 (1995) 864.
- [21] A.M. Stefanini, et al., Phys. Rev. C 73 (2006) 034606.
- [22] A.M. Stefanini, et al., Phys. Rev. C 65 (2002) 034609.
- [23] H. Timmers, et al., Phys. Lett. B 399 (1997) 35;
H. Timmers, et al., Nucl. Phys. A 633 (1998) 421.
- [24] M. Dasgupta, D.J. Hinde, N. Rowley, A.M. Stefanini, Annu. Rev. Nucl. Part. Sci. 48 (1998) 401.
- [25] K. Hagino, N. Rowley, A.T. Kruppa, Comput. Phys. Commun. 123 (1999) 143.
- [26] K. Hagino, private communication.
- [27] S. Raman, C.W. Nestor Jr., P. Tikkanen, At. Data Nucl. Data Tables 78 (2001) 1;
T. Kibédi, R.H. Spear, At. Data Nucl. Data Tables 80 (2002) 35.
- [28] Ö. Akyüz, Å. Winther, in: R.A. Broglia, R.A. Ricci (Eds.), Nuclear Structure and Heavy-Ion Physics, Proc. Int. School of Physics “Enrico Fermi”, Course LXXVII, Varenna, North-Holland, Amsterdam, 1981.
- [29] C.L. Jiang, et al., Phys. Rev. Lett. 93 (2004) 012701.